scientific reports

Check for updates

OPEN

GPER deficiency impedes murine myocutaneous revascularization and wound healing

Randy F. Ko[1], Oliver Q. C. Davidson[2], Michael A. Ahmed[2], Ross M. Clark[3,4], Jacquelyn S. Brandenburg[3], Vernon S. Pankratz[5], Geetanjali Sharma[1], Helen J. Hathaway[4,6], Eric R. Prossnitz[1,6,7,8]✉ & Thomas R. Howdieshell[2,8]✉

Estrogens regulate numerous physiological and pathological processes, including wide-ranging effects in wound healing. The effects of estrogens are mediated through multiple estrogen receptors (ERs), including the classical nuclear ERs (ERα and ERβ), that typically regulate gene expression, and the 7-transmembrane G protein-coupled estrogen receptor (GPER), that predominantly mediates rapid "non-genomic" signaling. Estrogen modulates the expression of various genes involved in epidermal function and regeneration, inflammation, matrix production, and protease inhibition, all critical to wound healing. Our previous work demonstrated improved myocutaneous wound healing in female mice compared to male mice. In the current study, we employed male and female GPER knockout mice to investigate the role of this estrogen receptor in wound revascularization and tissue viability. Using a murine myocutaneous flap model of graded ischemia, we measured real-time flap perfusion via laser speckle perfusion imaging. We conducted histologic and immunohistochemical analyses to assess skin and muscle viability, microvascular density and vessel morphology. Our results demonstrate that GPER is crucial in wound healing, mediating effects that are both dependent and independent of sex. Lack of GPER expression is associated with increased skin necrosis, reduced flap perfusion and altered vessel morphology. These findings contribute to understanding GPER signaling in wound healing and suggest possible therapeutic opportunities by targeting GPER.

17β-estradiol (E2) is the most potent and prevalent steroid estrogen hormone secreted by the ovaries. Estrogens regulate many essential physiological processes and are necessary for developing the reproductive system in females and males. The effects of estrogens are mediated through multiple estrogen receptors (ERs), including the classical nuclear ERs (ERα and ERβ), that typically regulate gene expression, and the 7-transmembrane G protein-coupled estrogen receptor (GPER), which predominantly mediates rapid "non-genomic" signaling. Over the past two decades, GPER has been identified as a regulator of various and diverse aspects of pathophysiology, including cardiovascular physiology and disease, metabolism (e.g., obesity and diabetes), multiple cancers, and inflammation (infection and inflammatory diseases), among others[1–5]. Emerging results demonstrate that estrogens play a significant role in human wound healing. Estrogen modulates numerous genes and processes involved in epidermal function and regeneration, inflammation, matrix production, and protease inhibition, all critical for effective wound repair[6].

Approximately 8.2 million Medicare recipients in the United States received wound care in 2018, with annual medical expenses for acute and chronic wound treatments ranging from $28 billion to $97 billion[7]. Gene expression studies reveal that impaired wound healing in humans is associated with increased age and is

[1]Division of Molecular Medicine, Department of Internal Medicine, University of New Mexico Health Science Center, Albuquerque, NM 87131, USA. [2]Department of Surgery, Augusta University/University of Georgia Medical Partnership, Athens, GA 30602, USA. [3]Department of Surgery, University of New Mexico Health Science Center, Albuquerque, NM 87131, USA. [4]Department of Cell Biology and Physiology, University of New Mexico Health Science Center, Albuquerque, NM 87131, USA. [5]Division of Epidemiology, Biostatistics, and Preventive Medicine Department of Internal Medicine, University of New Mexico Health Science Center, Albuquerque, NM 87131, USA. [6]University of New Mexico Comprehensive Cancer Center, University of New Mexico Health Science Center, Albuquerque, NM 87131, USA. [7]Center of Biomedical Research Excellence in Autophagy, Inflammation and Metabolism, University of New Mexico Health Science Center, Albuquerque, NM 87131, USA. [8]These authors jointly supervised this work: Eric R. Prossnitz and Thomas R. Howdieshell. ✉email: eprossnitz@salud.unm.edu; thowdieshell@augusta.edu

profoundly influenced by estrogen[6]. Clinically, as aging negatively affects wound healing, applying topical estrogen improved wound healing in older women and men, with increased collagen and fibronectin levels observed, leading to a reduction in wound size in both sexes[8]. In a human surgical wound study, increased collagen deposition was documented in premenopausal women compared to age-matched men[9]. In ovariectomized female mice, exogenous estrogen reversed the delay in acute incisional wound epithelialization in a model of cutaneous ischemia, potentially through increased expression of the anti-apoptotic Bcl-2 protein[10,11]. The beneficial effects of estrogen required ERα expression, as demonstrated by the lack of estrogen efficacy in ERα knockout (KO) mice[11]. Sex differences in the prevalence of skin wounds exist, with foot ulcers more common in men than women[12]. In addition, sexual dimorphism exists in endothelial cell function and angiogenesis[13]. Although GPER expression is higher in female versus male human umbilical vein endothelial cells (HUVEC), neither E2 nor G-1 enhanced HUVEC viability in cells derived from either sex[14]. In primary rat aortic vascular smooth muscle cells, GPER activation inhibits cell proliferation and migration and is downregulated during vascular injury[15]. Moreover, estrogen-induced angiogenesis in endothelial cells is mediated by GPER, involving key metabolic pathways[16]. In studies with triple-negative breast cancer cells, E2 suppressed vascular endothelial growth factor (VEGF) expression through GPER, reducing endothelial tube formation and angiogenesis[17]. Finally, we have shown in a murine myocutaneous flap model of graded ischemia that flap revascularization and healing are superior in female mice compared to male mice[18].

In this study, we utilized a GPER KO mouse model to determine whether GPER signaling plays a role in wound revascularization and repair. Employing the murine myocutaneous flap model of graded ischemia, we used laser speckle perfusion imaging (which provides depth-resolved blood flow measurements, typically limited to a depth of 300–500 μm) to assess perfusion throughout the flap[18]. Serial photography and planimetry were utilized to document gross flap viability. Image analysis followed histology and immunohistochemical staining to determine skin and muscle viability, microvascular density and vessel morphology. Our results using GPER KO mice demonstrate for the first time that GPER plays an essential role in wound healing, regardless of sex, showing that GPER expression is associated with increased neovascularization, perfusion, and flap viability. These findings advance the understanding of the role of GPER in wound healing and highlight the therapeutic potential of targeting this receptor.

Results

Our previous study demonstrated a sex difference in murine flap revascularization, with females exhibiting improved wound healing compared to males, suggesting a role for estrogen[18]. In a previous supporting publication, ovariectomy leads to a decline in wound healing, with the negative effect ameliorated by restoring estradiol after ovariectomy[11]. Although a role for ERα has been proposed,[11] we sought to determine whether GPER contributes to the differences observed in male and female murine wound healing by employing GPER KO in a murine myocutaneous flap model of wound healing.

GPER deficiency leads to increased fat and decreased dermal thickness in male mice

To explore the role of GPER in wound healing, we first examined the morphology of the skin and panniculus carnosus muscle in GPER KO and WT mice of both sexes. We and others have previously reported that GPER KO mice can exhibit limited metabolic dysfunction (e.g., weight gain) starting at six months of age[19]. As expected, there was no significant difference in weight observed between WT and GPER KO mice at the age used in this study (10 ± 2 weeks; Fig. 1a)[20]. Because the skin of female mice is thinner than that of males,[21,22] we sought to determine whether GPER expression affects skin morphology. Female WT mice exhibited an increased thickness of the subcutaneous fat layer and decreased dermal thickness compared to male WT mice (Fig. 1b).

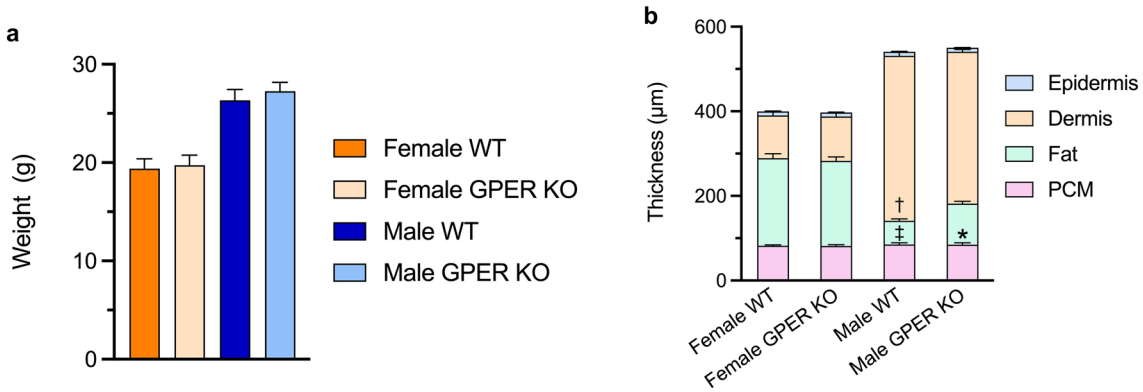

Figure 1. Effects of GPER deficiency on mouse body weight and skin morphology. (**a**) Age-matched female and male WT and GPER KO C57BL6 mice (10 ± 2 weeks of age) were weighed pre-operatively. $n = 15$ mice per group. (**b**) Epidermis, dermis, fat, and panniculus muscle (PCM) thickness was determined via image analysis of H&E-stained sections. $n = 5$ mice per group; ***P** < 0.0001 for male WT vs. GPER KO fat thickness, †$P < 0.0001$ for male WT vs female WT dermis thickness, ‡ $P < 0.0001$ for male WT vs. female WT fat thickness. PCM = panniculus carnosus muscle.

Moreover, while the overall morphology was not different when comparing female GPER KO to female WT mice, male GPER KO mice exhibited a significant increase in the thickness of the subcutaneous fat layer, with a commensurate decrease in dermal thickness, compared to male WT mice. (Fig. 1b).

GPER deficiency modulates temporal and spatial perfusion in the myocutaneous flap

Myocutaneous flap regions were evaluated before surgery (pre-op), immediately following surgery on postoperative day (POD) 0, and subsequently on days 2, 5, and 10, assessing skin perfusion within caudal, central, and cranial regions of interest (ROI) as described previously[18]. Immediately following surgery, perfusion initially dropped in all measured ROIs across all subgroups in a graded pattern, progressively declining towards the caudal region, with no differences observed between any of the four mouse groups (Fig. 2). The caudal region is the least perfused, displaying initial and ongoing ischemia, providing a stimulus for neovascularization.

As previously reported,[18] perfusion in female WT mice improved substantially on POD 2 in the cranial and central regions compared to the caudal region, with a sustained increase in caudal perfusion throughout the 10-day course. In male WT mice, although cranial perfusion on POD 2 was similar to females, perfusion then declined steadily through POD 10 (Fig. 2a). Overall, the central and caudal regions showed reduced perfusion in male WT mice compared to female WT mice at all but one time point (POD 2 in the caudal region; Fig. 2b).

In the cranial region of the flap, both male and female GPER KO mice showed a delay in peak perfusion, with maximal perfusion appearing on POD 5, compared to POD 2 in their WT counterparts, with a subsequent substantial decline by POD 10 in both sexes of GPER KO mice. Compared to WT mice, cranial perfusion was also greatly reduced on POD 2 in both male and female GPER KO mice. In both the central and caudal regions, perfusion in both male and female GPER KO mice was consistently lower than their WT counterparts at all time points except for females at POD 2 in the caudal region (Fig. 2b). In the caudal region, a progressive increase in perfusion over time was evident in female WT mice, surpassing the pre-operative baseline value by POD 10. In contrast, caudal perfusion in all other groups remained substantially below baseline levels.

GPER deficiency reduces flap viability

We also investigated the impact of GPER expression on flap viability (a function of perfusion) by evaluating the extent of externally visible cutaneous necrosis within the flap and the overall flap area (a measure of flap contraction, reflecting cutaneous and/or more profound panniculus muscle necrosis) (Fig. 3). On POD 2, 5,

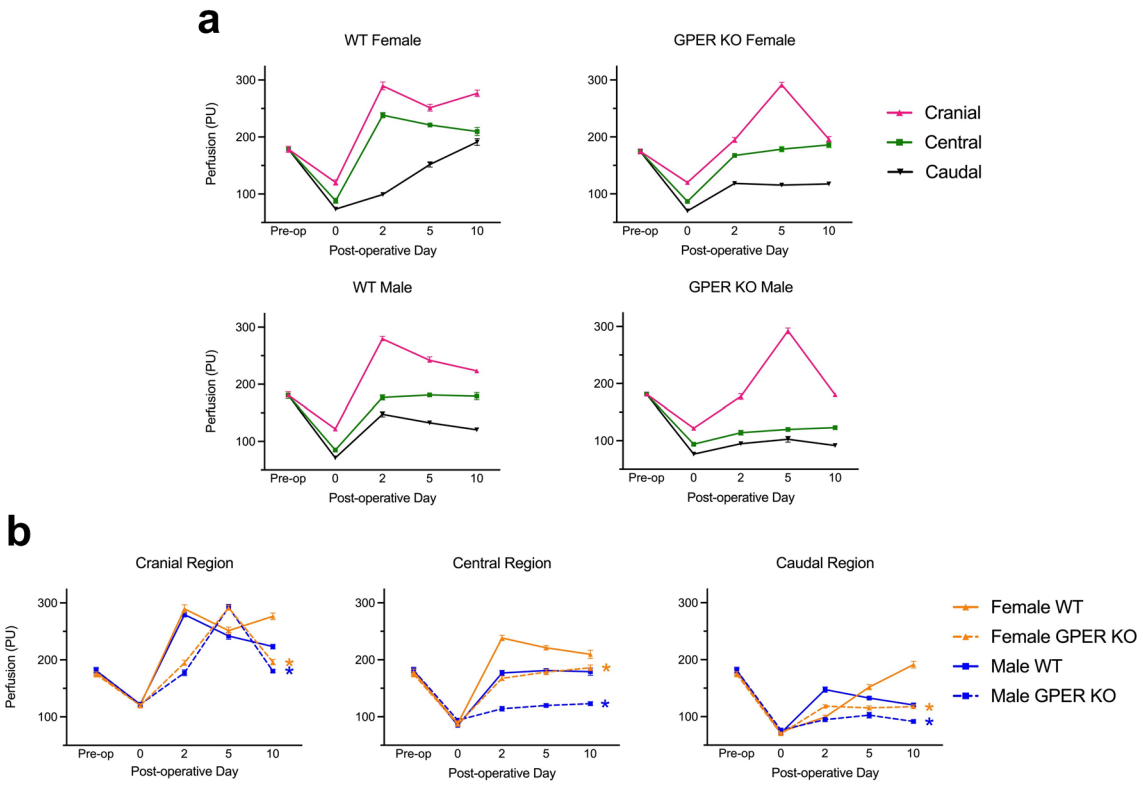

Figure 2. GPER deficiency leads to decreased perfusion in both sexes. Laser speckle perfusion imaging was performed on each mouse pre-operatively (Pre-op), immediately following surgery, and on postoperative day (POD), POD 2, POD 5, and POD 10 following surgery. Three regions of interest within the flap were imaged: cranial, central, and caudal. (**a**) Perfusion data are graphed based on genotype and sex. (**b**) The same perfusion data in (**a**) are graphed by flap region. $N = 10$ mice per group; $^{*}P < 0.05$ for GPER KO vs. WT mice on POD 10 (orange = female; blue = male). PU, perfusion units.

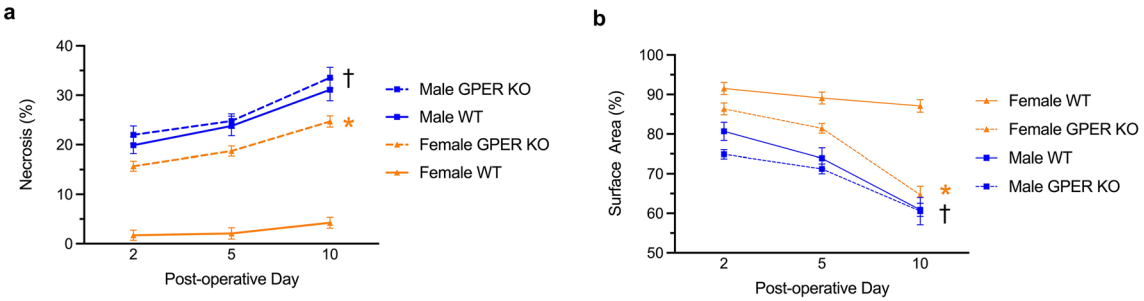

Figure 3. GPER deficiency increases flap necrosis and contraction. (**a**) Necrosis within the flap tissue of male and female WT and GPER KO mice on postoperative days (POD) 2, 5, and 10. (**b**) Flap area (a measure of contraction reflecting poor healing) was determined in male and female WT and GPER KO mice on postoperative days 2, 5, and 10 as a percentage relative to the initial flap. (**a, b**) $N = 10$ mice per group. $^*P < 0.0001$ for female WT vs. GPER KO mice on POD 10; $\dagger P < 0.0001$ for male GPER KO mice vs. female GPER KO mice on POD 10.

and 10, female GPER KO mice displayed a significant increase in flap necrosis (Fig. 3a), with a commensurate decrease in flap area (Fig. 3B), compared to their WT counterparts. Interestingly, male WT mice exhibited even greater flap necrosis and flap contraction than female GPER KO mice. However, the magnitude of the necrosis was not substantially increased in male GPER KO mice compared to male WT mice, as observed with female mice. Together, these results reveal that the limited flap necrosis and contraction observed in female WT mice is increased in both male WT mice and female GPER KO mice, suggesting an important role for both estrogen and GPER in maintaining myocutaneous wound healing. An effect of estrogen acting through other ERs in female GPER KO mice may contribute to the improved response in these mice compared to male WT or male GPER KO mice.

We also sectioned H&E-stained skin from the proximal and distal regions of the flap from all cohorts (isolated at sacrifice on POD 10), and the spatial effects of graded ischemia on tissue viability and morphology were further assessed by histological evaluation (Fig. 4). H&E staining of the proximal and distal flap morphology at POD 10 revealed differences in tissue viability and morphology between GPER KO mice and their respective sex-matched WT counterparts (Fig. 4). Complete proximal flap viability was evident in all groups (Fig. 4a–d). However, flaps from female WT and GPER KO mice (Figs. 4a, c) had reduced dermal and increased hypodermal composition compared to flaps from male WT and GPER KO mice (Figs. 4b, d).

With respect to distal flap histology (Fig. 4e–h), female WT mice exhibited full-thickness viability, including epidermis, dermis, hypodermis, and panniculus carnosus muscle with adherent granulation tissue (Fig. 4e). In contrast, female GPER KO distal flap histology confirmed dermal and panniculus carnosus muscle necrosis and viable epidermis (Fig. 4g). Distal male WT flap histology displayed a transition from flap necrosis to viable adjacent wound margins (Fig. 4f), with an absence of viable dermis and panniculus carnosus muscle in the necrotic portion, and proliferative epidermis closing the wound by secondary intention. Male GPER KO distal flap histology revealed extensive necrosis of the epidermis, dermis, hypodermis, and panniculus muscle (Fig. 4h).

GPER deficiency decreases muscle viability in both sexes

To further investigate GPER's role in myocutaneous flap wound healing, we evaluated the viability of the panniculus carnosus muscle in male and female GPER KO mice and their corresponding WT counterparts. Both male and female WT mice maintained significantly greater muscle viability compared to their corresponding GPER KO counterparts (Fig. 5). Although female WT mice exhibited substantially greater muscle viability than male WT mice, both male and female GPER KO mice showed significantly lower muscle viability compared to their corresponding WT counterparts. The protective effect of the female sex in WT female mice was reduced by almost half in female GPER KO mice, which was similar to the magnitude observed in male WT mice. In addition, female GPER KO mice displayed significantly higher muscle viability than male GPER KO mice, revealing a continued sex dependence even in GPER KO mice. Together, these results show that muscle viability in this model depends greatly on sex and GPER expression in both sexes.

GPER deficiency reduces microvascularity

Microvascular anatomy was analyzed in control mice and at POD 10 in experimental mice in the proximal and distal regions of the flap. CD-31 immunostaining was followed by digital image analysis to determine the microvascular density (i.e., the number of vessels per mm^2) and total vessel area (which incorporates both the number and size of vessels; Figs. 6 and 7), reflecting distal neovascularization and proximal arteriogenesis respectively following the hypoxic conditions introduced by the creation of the flap.

In proximal flaps, there was no change in vessel count in any of the groups (Fig. 6a–d, Fig. 7a); however, all groups showed a change in vessel morphology (Fig. 7b), with enlarged vessel diameter and therefore area (i.e., arteriogenesis), compared to control vessel diameter. Both female WT and GPER KO mice exhibited increased vessel areas compared to their male counterparts, which were nevertheless increased compared to their corresponding control tissues. In addition, both female and male GPER KO mice displayed reduced vessel

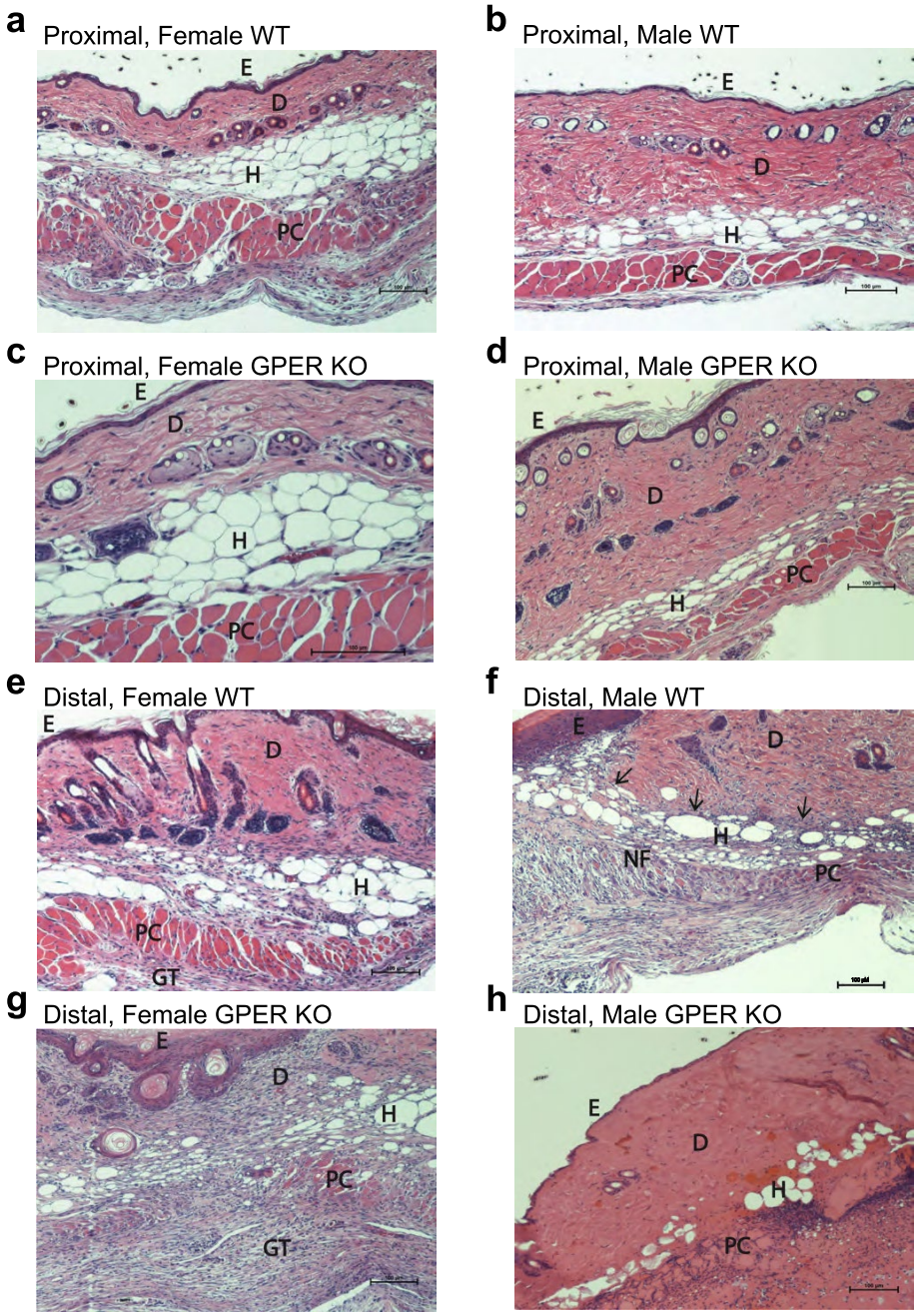

Figure 4. Histological evaluation of proximal and distal flap morphology. The effect of graded ischemia on tissue viability and flap morphology was evaluated using H&E-stained sections from female and male WT and GPER KO mice on POD 10. Representative images of proximal flaps from (**a**) Female WT mice, (**b**) Male WT mice, (**c**) Female GPER KO mice, and (**d**) Male GPER KO mice. Representative images of distal flaps from **(e)** Female WT, (**f**) Male WT illustrating the junction between the viable flap and the necrotic flap area, demarcated by the wound margin (arrows), (**g**) Female GPER KO, and (**h**) Male GPER KO mice. Scale bars in all images represent 100 μm. Labels: epidermis (E), dermis (D), hypodermis (subcutaneous fat) (H), panniculus carnosus muscle (PC), a necrotic portion of the flap (NF), and granulation tissue (GT). GPER = G protein-coupled estrogen receptor.

area compared to their WT counterparts. Interestingly, female GPER KO mice showed an increased vessel area compared to male WT mice, suggesting other estrogen-mediated contributing factors in female mice (Fig. 7).

In contrast, in the distal flap, only female WT mice exhibited new vessel growth (neovascularization) into the flap muscle and fat (Fig. 6e), with an increase in vessel count and vessel area compared to female GPER KO mice (Fig. 7). The similar magnitude of increase in each parameter in female WT mice suggests that the increased vessel count (2.7-fold) likely accounts for the majority of the increase observed in vessel area (2.9-fold). Female

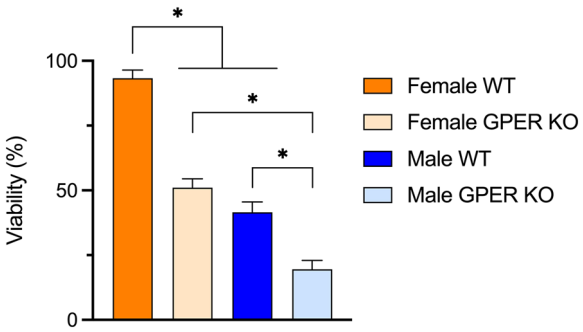

Figure 5. GPER deficiency reduces muscle viability in male and female mice. Muscle viability at POD 10 was quantified via image analysis of (**H** and **E**)-stained sections. $^{*}p < 0.0001$ between representative comparison groups.

GPER KO mice displayed new blood vessel growth within scattered viable panniculus carnosus muscle bundles but with uniform flap necrosis of the epidermis, dermis, and fat (Fig. 6g). Male WT mice exhibited prominent new vasculature solely in the granulation tissue beneath the avascular necrotic distal flap (Fig. 6f). However, both male WT and GPER KO mice exhibited a slight reduction in vessel count and area compared to their respective non-operative controls (Fig. 7). Male GPER KO mice showed healthy lateral wound margins and avascular full-thickness flap necrosis in distal flap sections (Fig. 6h). Both female and male vessel parameters are consistent with the POD 10 caudal perfusion data (Fig. 2b), showing selectively improved perfusion in female WT mice. Together, these results suggest that GPER expression plays a critical role in neovascularization in the most hypoxic distal flap region.

Discussion

In the current study, we establish that GPER plays a crucial role in myocutaneous wound healing and revascularization, regardless of sex, albeit with more pronounced effects in females. When comparing GPER-deficient mice with their WT counterparts, we observed considerable spatial and temporal differences in perfusion within the flap. This impaired perfusion, as a consequence of GPER deficiency, may result in increased flap cutaneous necrosis and reduced panniculus muscle viability observed in GPER KO mice. However, the direct effects of GPER expression on cutaneous and muscle viability cannot be excluded[23]. Furthermore, GPER-deficient mice displayed altered angiogenic responses, indicating a potential role for GPER in modulating the formation and maintenance of new blood vessels during the wound healing process. These discoveries of GPER have profound implications for understanding the complex interplay between hormones, the immune system, and vascular biology.

GPER KO mice have been an essential tool in revealing the functions of GPER in numerous physiological and pathophysiological areas, including cardiovascular, endocrine, reproductive, immune, and musculoskeletal systems, among others[2,24]. GPER KO mice exhibit increased adiposity, impaired insulin secretion from pancreatic islets, and an obesity-related phenotype marked by insulin resistance and glucose intolerance compared to WT mice[19,20,25,26]. Insulin promotes tissue repair and regulates several cellular processes involved in wound healing, including cell migration, proliferation, and angiogenesis[27]. In wound healing, GPER's role in modulating insulin secretion may become increasingly important under hypoxic conditions, as insulin promotes tissue repair and angiogenesis[28]. GPER expression has been shown to have a functional interaction with hypoxia-inducible factor-1α (HIF-1α), resulting in the positive regulation of VEGF under hypoxic conditions, which can further affect angiogenesis and tissue repair processes[29]. Understanding the interplay between GPER, insulin secretion, and hypoxia may provide valuable insights into developing therapeutic strategies to improve wound healing outcomes, especially in individuals with compromised tissue repair, such as those with obesity or diabetes[28]. Interestingly, diet-induced obese mice exhibited reduced myocutaneous perfusion, microvascular density, and distal flap revascularization compared to WT controls, underscoring the importance of exploring the potential role of estrogen-mediated GPER signaling in these processes[30]. In line with previous studies, we observed no overt obesity in 10 ± 2-week-old GPER KO mice overall; however, we did find an increase in the hypodermis in male GPER KO mice compared to their WT counterparts, suggesting the possibility of underlying metabolic dysfunction[31]. The interplay between GPER signaling, insulin secretion, and hypoxic conditions highlights the complex regulatory networks influencing wound healing and revascularization.

This study highlights the pivotal role of GPER expression in revascularization in both male and female mice, especially in the ischemic distal flap region, as evidenced by increases in vessel density and area among female WT mice compared to female GPER KO mice. In males, WT mice show an increase in the proximal vessel area compared to GPER KO mice. Our findings suggest that GPER improves perfusion in both sexes throughout the flap, highlighting its significance in wound healing and angiogenesis. GPER activation is known to stimulate endothelial nitric oxide synthase (eNOS) and nitric oxide production, consequently mediating a range of protective cardiovascular effects[32]. Additionally, GPER activation enhances VEGF production in fibroblasts by upregulating HIF-1α, promoting endothelial tube formation[33]. GPER also governs estrogen-induced maintenance of endothelial tube formation that fails under hypoxia/reoxygenation conditions through eNOS and

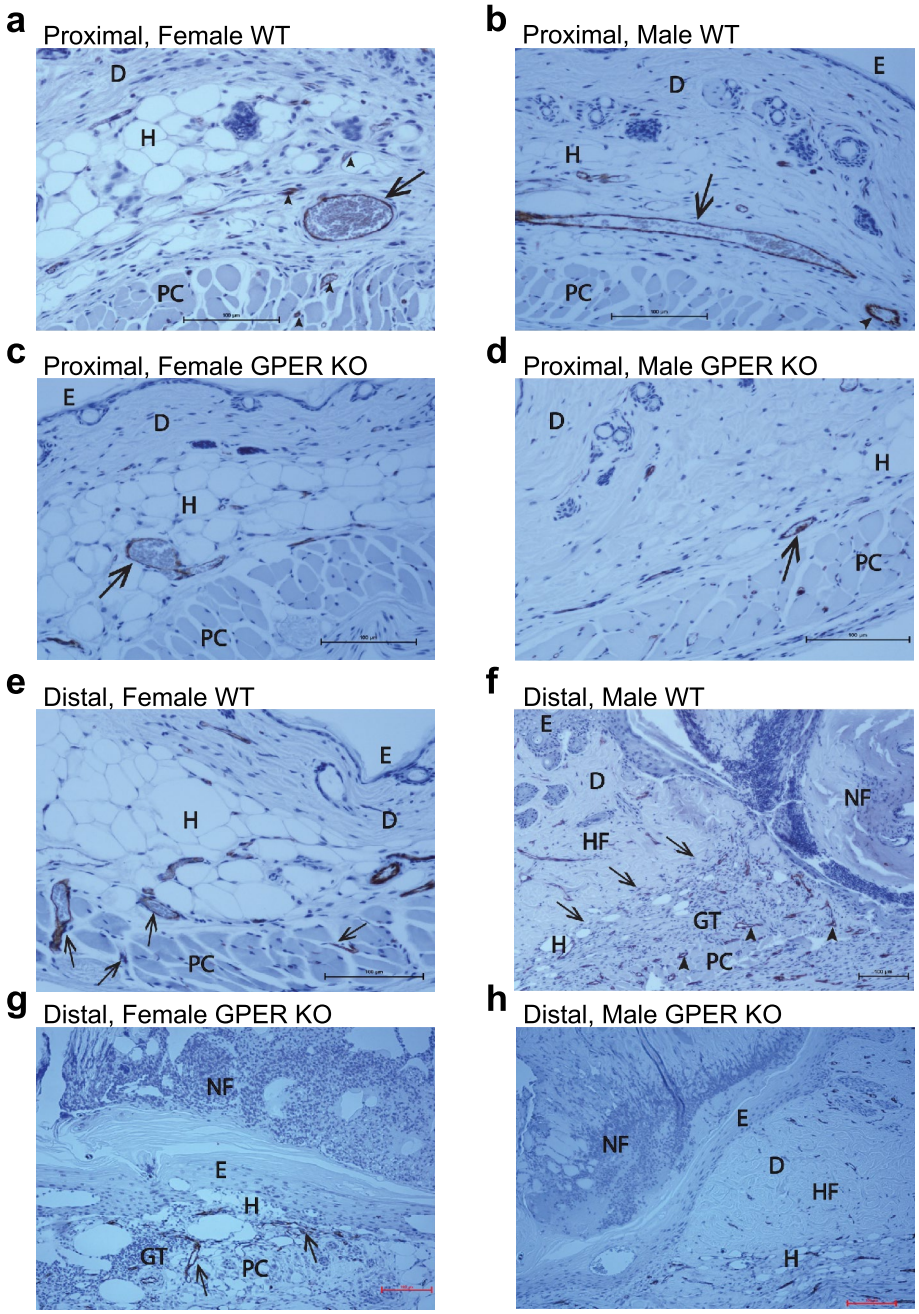

Figure 6. CD-31 immunostaining of proximal and distal flap histologic sections to assess blood vessel location, density, and lumen size. Day 10 proximal flap histology in female and male WT and GPER KO mice revealed enlarged blood vessels consistent with arteriogenesis (a-d). Representative images of proximal flap sections from (**a**) Female WT showing a markedly enlarged blood vessel (arrow) in the subcutaneous fat, compared to other vessels (arrowheads) in the subcutaneous tissue or within bundles of the panniculus muscle. (**b**) Male WT with large subcutaneous blood vessels (arrow) in longitudinal and axial views. (**c**) Female GPER KO demonstrating a large subcutaneous blood vessel (arrow). (**d**) Male GPER KO exhibiting uniform tissue viability and limited enlargement of a subcutaneous vessel (arrow). Representative images of distal flap sections (**e**–**h**) from (**e**) Female WT with viable epidermis, dermis, hypodermis, and panniculus muscle, and new vessel growth into flap muscle and fat (arrows). (**f**) Male WT at the junction of the healthy lateral wound and necrotic flap margin (arrows), revealing prominent new vasculature (arrowheads) solely in the granulation tissue beneath the avascular necrotic flap. (**g**) Female GPER KO with limited new blood vessel growth (arrows) within scattered viable panniculus carnosus muscle bundles and uniform flap necrosis of epidermis, dermis, and fat. (**h**) Male GPER KO showing healthy lateral wound margin and avascular full-thickness flap necrosis. Scale bars in all images represent 100 μm. The labels are denoted as follows: the epidermis (E), dermis (D), hypodermis (subcutaneous fat) (H), panniculus carnosus muscle (PC), healthy flap lateral wound (HF), necrotic flap margin (NF), and granulation tissue (GT). GPER = G protein-coupled estrogen receptor.

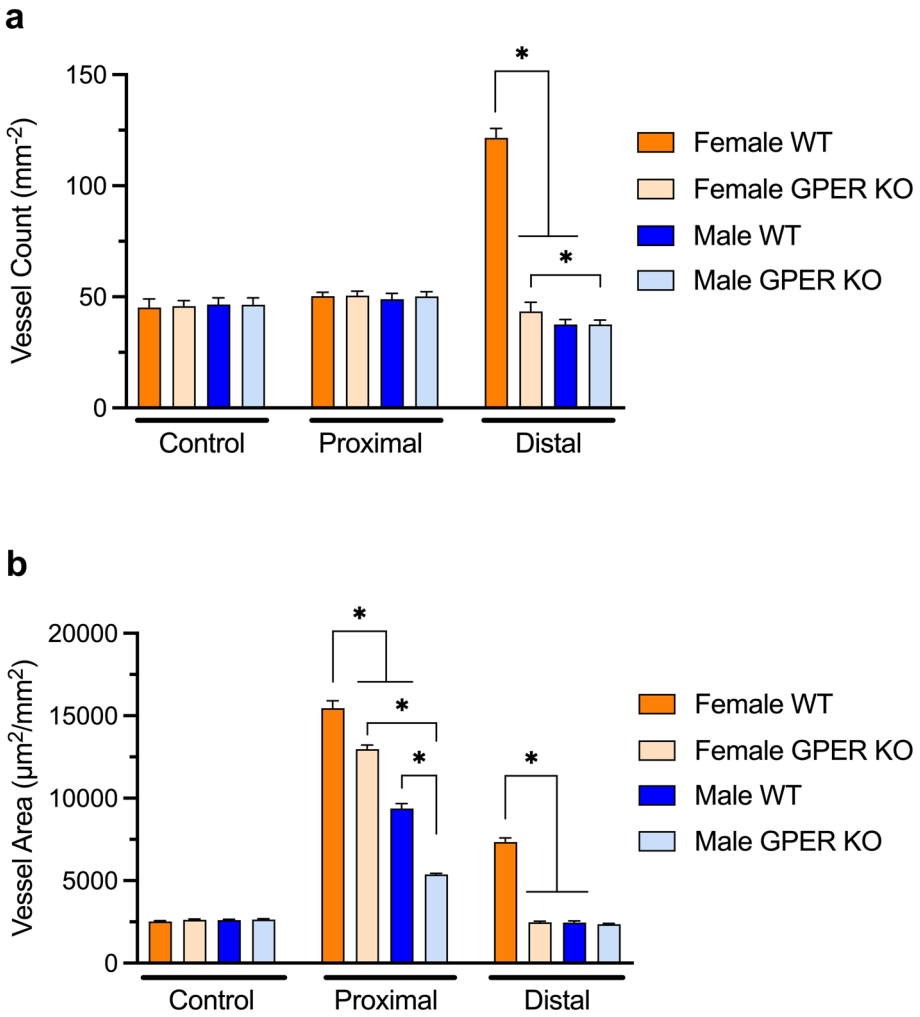

Figure 7. GPER deficiency decreases microvascularity in distal and proximal regions. Analysis of vessel parameters in female and male WT and GPER KO mice in control skin and proximal and distal flap regions for: (**a**) microvascular density (vessel count) and (**b**) vessel morphology (vessel area). $N = 5$ mice per group for controls and $n = 10$ mice per group for proximal and distal flaps. $^{*}P < 0.0001$ for comparison between respective groups.

Akt activation[34]. Our findings highlight the essential role of GPER in regulating perfusion and revascularization during the wound healing process, regardless of sex.

The effects of estrogen on the skin and in wound healing are well-established in both humans and mice. Indeed, in the early stages of menopause (within the first five years), there is a notable 30% decrease in the levels of collagen types I and III, which are crucial for maintaining skin integrity and structure[35]. From a clinical standpoint, the age-related decline in wound healing efficacy can be mitigated by applying topical estrogen, which has been shown to enhance wound healing in both older women and men[8]. In an ovariectomized mouse model of cutaneous ischemia, either estrogen or tamoxifen treatment reduced skin ischemia by promoting reperfusion with increased expression of antiapoptotic Bcl-2, fibroblast growth factor-2 (FGF2) and VEGF[11]. The estrogen-mediated protective effects were absent in estrogen receptor α deficient (ER α KO) mice[11]. However, in stark contrast to the impaired wound healing observed in female GPER KO mice in this study, female ERα KO mice exhibited no compromised wound recovery, underscoring the distinct roles of these respective receptors in the wound healing process[11]. Furthermore, our previous study found that FGF2 and Notch1 local gene expression were both increased in female mice compared to male mice[18]. There is a substantial reduction in neovascularization observed in ovariectomized mice, despite the presence of FGF2, which highlights the crucial role of estradiol in amplifying angiogenesis[36]. Additionally, E2 can mediate Notch1 activation, contributing to the protective effects of VEGF on endothelial cells and promoting their survival[37]. The reduced wound revascularization and increased necrosis observed in GPER KO mice may be attributed to the lack or alteration of one or more GPER-mediated activities, including but not limited to FGF2 and Notch1. These findings highlight the importance of GPER expression and sex differences (including estrogen action) in vascular biology, opening up new avenues for research into mechanisms governing microvascularity.

Inflammation is a critical component of wound healing, and GPER is expressed in multiple immune cells, including T-lymphocytes, B-lymphocytes, monocytes, macrophages, eosinophils, and neutrophils[38]. While an optimal level of inflammation is essential, conditions such as pyoderma gangrenosum exemplify the detrimental effects of excessive inflammation, which can be managed effectively through immune suppression[39]. Thus, a balanced inflammatory response is essential during wound healing. GPER KO mice exhibit an enhanced proinflammatory phenotype characterized by increased cytokine production, highlighting GPER's potential role in modulating inflammation[19]. GPER is involved in various immune functions, demonstrated by its sufficiency and necessity for estradiol-mediated protection in a murine experimental autoimmune encephalomyelitis model of multiple sclerosis[40]. Estrogen also modulates immune responses by downregulating the macrophage migration inhibitory factor, affecting cell migration, immune cell recruitment, and angiogenesis, essential elements of wound healing[10,41]. GPER, in its multifunctional role within neutrophils, increases the expression of IL1β, CXCL8, and COX2, enhances respiratory burst, extends lifespan, and demonstrates anti-inflammatory effects[42]. Macrophages play a pivotal role in wound healing, bridging inflammatory and reparative phases by clearing debris and initiating the repair[30,43]. The activation of GPER via G-1 inhibits the production of proinflammatory cytokines and chemokines, including PGE2, TNF-α, IL-12, IL-6, and CCL5, by monocytes and macrophages, suggesting GPER's potential to mitigate excessive inflammation and promote a favorable tissue repair milieu[44,45]. Taken together, the literature underscores the dynamic role of GPER in modulating immune cell functions and inflammatory responses during wound healing.

Foxp3-expressing T_{regs} are important in wound healing, promoting epidermal regeneration, and preventing dermal fibrosis[46]. Estrogen promotes transforming growth factor (TGF-β) secretion, which is essential in angiogenesis, re-epithelialization, inflammation, and granulation tissue formation during wound healing[47,48]. TGF-β functions as a unifying molecule in facilitating the differentiation and survival of regulatory T-cell phenotype (T_{reg})-cell precursors by antagonizing thymic-negative selection[49]. GPER activation induces T_{reg}-cells, while TGF-β modulates naive $CD4^+$ T cells differentiation into T_{regs}[40]. Previous findings have shown that G-1, a GPER agonist, can stimulate Foxp3 and IL10 expression, two essential regulatory T cell markers[50,51]. Consequently, GPER expression modulation of regulatory T cells may have significant implications for wound healing biology, emphasizing the need for further research.

In summary, our study emphasizes the essential function of GPER in modulating myocutaneous wound healing and revascularization, irrespective of sex, and highlights its pronounced effects in females. We have shown that GPER deficiency results in delayed peak perfusion, decreased functional revascularization, diminished microvascular density, and increased flap necrosis in mice, demonstrating its significance in these processes. The observed sex differences in vascular biology and GPER expression emphasize the need to thoroughly investigate such differences when designing intervention strategies for clinical applications. The potential modulation of GPER activity may have important implications in developing novel therapeutic approaches to enhance wound healing outcomes, particularly in populations with heightened susceptibility to impaired healing, such as individuals with obesity, diabetes, and ischemia, among others. Further research into the precise molecular mechanisms of GPER-mediated effects in the context of wound healing and vascular biology will advance our understanding of these complex processes and provide new avenues for developing targeted treatments to improve the quality of life for patients with compromised wound healing.

Materials and methods

Mouse models and care

Wild type (WT) C57BL/6 and GPER KO mice were housed at the Animal Resource Facility of the University of New Mexico (UNM) Health Sciences Center under controlled temperature (22-23°C) on a 12-h light–dark cycle with unrestricted access to standard chow and water. GPER KO mice (provided by J. S. Rosenbaum, Procter & Gamble Co.) were generated as previously described and backcrossed 10 generations onto the C57BL/6 background (Harlan Laboratories)[40]. All procedures were approved by the Institutional Animal Care and Use Committee of the UNM Health Sciences Center and carried out under UNM institutional policies and the National Institutes of Health (NIH) Guide for the Care and Use of Laboratory Animals. All methods were carried out in accordance with relevant guidelines and regulations. This study is reported in accordance with ARRIVE guidelines, with no exclusions of mice in the analysis, and the exceptions noted below.

Mouse myocutaneous flap model and wound morphology analysis

Aged-matched female and male WT and GPER KO C57BL6 mice (10 ± 2 weeks of age) underwent anesthesia with isoflurane (1–3%) via nose cone inhalation. A total of 60 mice were used in the study, including 10 male WT, 10 female WT, 10 male GPER KO, and 10 female GPER KO mice that underwent flap surgery. Although blinding was not performed, randomization of mice to experimental groups (WT versus KO, and male versus female) was driven by Mendelian inheritance. In addition, 5 male WT, 5 female WT, 5 male GPER KO, and 5 female GPER KO mice were incorporated into the study as nonoperative tissue controls. All mice were weighed pre-operatively and on postoperative day (POD) 10.

Under inhalation anesthesia, the dorsal surface was depilated using electric clippers (mice displaying nevi, which interferes with light reflection, were excluded and another mouse selected at random), and the site was prepped with povidone-iodine and 70% ethanol. A peninsular flap (3 cm long and 1.5 cm wide) of skin, adipose tissue, and panniculus carnosus muscle was surgically created by making three soft tissue incisions. Precise flap dimensions were confirmed by projecting a laser template and measuring with a caliper[30]. The flap was elevated cranially and re-approximated at the edges with 6–0 monofilament sutures. Postoperative analgesia was provided using a single subcutaneous dose (0.01 mg/kg) of buprenorphine hydrochloride. After surgery, each animal was housed independently and received water and food ad libitum.

At 0 (immediately following flap surgery), 2, 5, and 10 days post-surgery, the dorsal flap was photographed for image analysis using a Nikon D70 digital camera (Nikon Instruments, Melville, New York), which was equipped with a macro lens and mounted on a tripod at a consistent height. The total flap area was computed using a standard planimetry method. The percentage of visible flap necrosis was calculated by dividing the measured necrotic area by the total flap area on each measurement day.

Laser speckle perfusion imaging

Each animal underwent inhalation anesthesia in a prone position at 0 h, 2 days, 5 days, and 10 days after surgery. Laser speckle perfusion imaging was performed with the full-field laser perfusion imager (moorFLPI, Moor Instruments, Essex, UK) in low-resolution/high-speed setting at a display rate of 25 Hz, time constant of 1.0 s and camera exposure time of 20 ms. The instrument head containing the charged coupled device (CCD) camera was positioned 30 cm above the mouse's back skin tissue surface using an articulating arm. The contrast images were processed to produce a scaled color-coded live flux image (red, high perfusion; blue, low perfusion), which correlated with the blood flow velocity in the tissue. Real-time data were acquired in the live image measurement mode.

The FLPI instrument reports perfusion in arbitrary units. The image was calibrated to assign values to a measurement using a reference flux signal generated by the laser light scattered from a suspension of polystyrene microspheres in water undergoing thermal or Brownian motion. From kinetic theory, the average velocity of the microspheres is proportional to the square root of the temperature in Kelvin. All measurements were performed at a room temperature of 20°C[52].

For each time point examined, 10 single-frame images acquired at end-expiration (no torso movement) were analyzed in the repeat image measurement window using three identical regions of interest (ROI): cranial, central, and caudal. The mean perfusion in each ROI was calculated for control skin and the peninsular flaps at each time point[53].

Tissue harvest, histology, and immunochemical staining

Mice without surgery (utilized as tissue controls) or 10 days following flap surgery were humanely euthanized by CO_2 inhalation for tissue collection and histologic examination. Unoperated back skin (controls) or POD 10 flap tissue was excised using sterile technique and transversely bisected, yielding proximal and distal tissue specimens. Histology samples were processed in two flap regions (proximal and distal) rather than three ROIs analyzed for perfusion imaging. The tissue was fixed in IHC Zinc Fixative (BD Biosciences-Pharmingen, San Diego, California) for 24 h, processed, and paraffin-embedded. Serial Sects. (4 μm) were dewaxed in xylene and gradually hydrated through graded ethanol and phosphate-buffered saline solution before staining with hematoxylin and eosin (H&E; Vector Laboratories, Burlingame, California) for the determination of skin morphology and panniculus muscle viability or CD-31 immunohistochemistry for the determination of blood vessel density and morphology.

Blood vessel density and morphology were determined by CD-31 immunostaining. After dewaxing and hydration, sections were incubated for 10 min in 3% hydrogen peroxide in methanol to block endogenous peroxidase activity, washed in phosphate-buffered saline, and incubated with primary antibody (rat anti-mouse CD-31, 1:50, BD Biosciences-Pharmingen) for 1 h at room temperature in a humidified chamber. Next, the sections were incubated with a biotinylated secondary antibody (anti-rat immunoglobin horseradish peroxidase kit, 1:50, BD Biosciences-Pharmingen) for 30 min at room temperature. The streptavidin–horseradish peroxidase reagent was applied for 30 min, followed by 3,3'-diaminobenzidine (DAB) chromogen for 5 min. With quick immersion, the sections were counterstained with Vector Hematoxylin QS (Vector Laboratories). The DAB substrate-chromogen resulted in a brown-colored precipitate at the antigen site.

Panniculus muscle viability and vessel density and morphology determination

Multiple full-thickness male and female nonoperative control tissue sections and POD 10 male and female flap biopsy sections (three proximal and three distal sections per mouse) were stained as above and analyzed. A Zeiss microscope with an attached digital camera (Carl Zeiss Microimaging, Jena, Germany) was used for image acquisition. Magnified images (× 100) were analyzed with SlideBook image analysis software (SlideBook 5.0; Intelligent Imaging Innovations, Santa Monica, California). Muscle viability (muscle area index) was determined with H&E-stained sections by dividing the viable panniculus carnosus muscle area from POD 10 distal sections by the muscle area on unoperated, control H&E-stained distal sections. Vessel density (vessel count per mm^2) and vessel morphology (vessel area reflecting both vessel count and size; $\mu m^2/mm^2$) were determined with image analysis of CD-31 immunostained Sects.[30,53]. Both vessel density and morphology were analyzed in the flap, and granulation tissue was excluded from the study.

Statistical analysis

Statistical analysis was performed with SAS (Cary, NC, version 9.4). Differences among groups and between baseline and subsequent time points were determined by analysis of variance approaches. Repeated-measures methods and data transformations were utilized when necessary. Fisher's Protected Least Significant Difference tests were used for post hoc analysis, with pairwise comparisons being evaluated for significance only if the global test for the factor combination of interest reached statistical significance[54]. All data are expressed as mean ± standard error of the mean (SEM). A 2-sided p-value of less than 0.05 was considered statistically significant. A comprehensive analysis of all cross-comparisons is available in the supplementary data (Supplementary information 1).

Data availability

Data are provided within the manuscript or supplementary information files.

Received: 1 February 2024; Accepted: 25 July 2024
Published online: 08 August 2024

References

1. Nilsson, S. *et al.* Mechanisms of estrogen action. *Physiol. Rev.* **81**, 1535–1565 (2001).
2. Prossnitz, E. R. & Barton, M. The G-protein-coupled estrogen receptor GPER in health and disease. *Nat. Rev. Endocrinol.* **7**, 715–726 (2011).
3. Barton, M. *et al.* Twenty years of the G protein-coupled estrogen receptor GPER: Historical and personal perspectives. *J. Steroid Biochem. Mol. Biol.* **176**, 4–15 (2018).
4. Meyer, M. R. & Barton, M. GPER blockers as Nox downregulators: A new drug class to target chronic non-communicable diseases. *J. Steroid Biochem. Mol. Biol.* **176**, 82–87 (2018).
5. Arterburn, J. B. & Prossnitz, E. R. G protein-coupled estrogen receptor GPER: Molecular pharmacology and therapeutic applications. *Annu. Rev. Pharmacol. Toxicol.* **63**, 295–320 (2023).
6. Hardman, M. J. & Ashcroft, G. S. Estrogen, not intrinsic aging, is the major regulator of delayed human wound healing in the elderly. *Genome Biol.* **9**, R80 (2008).
7. Sen, C. K. Human wounds and its burden: An updated compendium of estimates. *Adv. Wound Care* **8**, 39–48 (2019).
8. Ashcroft, G. S., Greenwell-Wild, T., Horan, M. A., Wahl, S. M. & Ferguson, M. W. J. Topical estrogen accelerates cutaneous wound healing in aged humans associated with an altered inflammatory response. *Am. J. Pathol.* **155**, 1137–1146 (1999).
9. Jorgensen, L. N., Sorensen, L. T., Kallehave, F., Vange, J. & Gottrup, F. Premenopausal women deposit more collagen than men during healing of an experimental wound. *Surgery* **131**, 338–343 (2002).
10. Coloma, M. J. & Morrison, S. L. Estrogen accelerates cutaneous wound healing associated with an increase in TGF-beta1 levels. *Nat. Med.* **27**, 159–163 (1990).
11. Toutain, C. E. *et al.* Prevention of skin flap necrosis by estradiol involves reperfusion of a protected vascular network. *Circ. Res.* **104**, 245–254 (2009).
12. Zhang, P. *et al.* Global epidemiology of diabetic foot ulceration: A systematic review and meta-analysis. *Ann. Med.* **49**, 106–116 (2017).
13. Cignarella, A. *et al.* Clinical efficacy and safety of angiogenesis inhibitors: Sex differences and current challenges. *Cardiovasc. Res.* **118**, 988–1003 (2022).
14. Boscaro, C. *et al.* Sex differences in the pro-angiogenic response of human endothelial cells: Focus on PFKFB3 and FAK activation. *Front. Pharmacol.* **11**, 587221 (2020).
15. Gros, R. *et al.* Extent of vascular remodeling is dependent on the balance between estrogen receptor α and G-protein-coupled estrogen receptor. *Hypertens. Dallas Tex* **1979**(68), 1225–1235 (2016).
16. Trenti, A. *et al.* The glycolytic enzyme PFKFB3 is involved in estrogen-mediated angiogenesis via GPER1. *J. Pharmacol. Exp. Ther.* **361**, 398–407 (2017).
17. Wang, C. *et al.* Oestrogen Inhibits VEGF expression and angiogenesis in triple-negative breast cancer by activating GPER-1. *J. Cancer* **9**, 3802–3811 (2018).
18. Brandenburg, J. S. *et al.* Sex differences in murine myocutaneous flap revascularization. *Wound Repair Regen* **28**, 1–10 (2020).
19. Sharma, G. *et al.* GPER deficiency in male mice results in insulin resistance, dyslipidemia, and a proinflammatory state. *Endocrinology* **154**, 4136–4145 (2013).
20. Haas, E. *et al.* Regulatory role of G protein-coupled estrogen receptor for vascular function and obesity. *Circ. Res.* **104**, 288–291 (2009).
21. Firooz, A. *et al.* The influence of gender and age on the thickness and echo-density of skin. *Skin Res. Technol.* **23**(1), 13–20 (2017).
22. Azzi, L., El-Alfy, M., Martel, C. & Labrie, F. Gender differences in mouse skin morphology and specific effects of sex steroids and dehydroepiandrosterone. *J. Invest. Dermatol.* **124**, 22–27 (2005).
23. Collins, B. C. *et al.* Deletion of estrogen receptor α in skeletal muscle results in impaired contractility in female mice. *J. Appl. Physiol. Bethesda Md* **1985**(124), 980–992 (2018).
24. Prossnitz, E. R. & Hathaway, H. J. What have we learned about GPER function in physiology and disease from knockout mice?. *J. Steroid Biochem. Mol. Biol.* **153**, 114–126 (2015).
25. Mårtensson, U. E. A. *et al.* Deletion of the G protein-coupled receptor 30 impairs glucose tolerance, reduces bone growth, increases blood pressure, and eliminates estradiol-stimulated insulin release in female mice. *Endocrinology* **150**, 687–698 (2009).
26. Sharma, G. & Prossnitz, E. R. Targeting the G protein-coupled estrogen receptor (GPER) in obesity and diabetes. *Endocr. Metab. Sci.* **2**, 100080 (2021).
27. Liu, Y., Petreaca, M. & Martins-Green, M. Cell and molecular mechanisms of insulin-induced angiogenesis. *J. Cell. Mol. Med.* **13**, 4492–4504 (2009).
28. Pierpont, Y. N. *et al.* Obesity and surgical wound healing: A current review. *ISRN Obes.* **2014**, 638936 (2014).
29. De Francesco, E. M. *et al.* GPER mediates the angiocrine actions induced by IGF1 through the HIF-1α/VEGF pathway in the breast tumor microenvironment. *Breast Cancer Res.* **19**, 129 (2017).
30. Clark, R. M., Coffman, B., McGuire, P. G. & Howdieshell, T. R. Myocutaneous revascularization following graded ischemia in lean and obese mice. *Diabetes Metab. Syndr. Obes. Targets Ther.* **9**, 325–336 (2016).
31. Davis, K. E. *et al.* Sexually dimorphic role of G protein-coupled estrogen receptor (GPER) in modulating energy homeostasis. *Horm. Behav.* **66**, 196–207 (2014).
32. Fredette, N. C., Meyer, M. R. & Prossnitz, E. R. Role of GPER in estrogen-dependent nitric oxide formation and vasodilation. *J. Steroid Biochem. Mol. Biol.* **176**, 65–72 (2018).
33. De Francesco, E. M. *et al.* GPER mediates activation of HIF1α/VEGF signaling by estrogens. *Cancer Res.* **74**, 4053 (2014).
34. Zhou, L. *et al.* G-protein-coupled receptor 30 mediates the effects of estrogen on endothelial cell tube formation in vitro. *Int. J. Mol. Med.* **39**(6), 1461–1467 (2017).
35. Affinito, P. *et al.* Effects of postmenopausal hypoestrogenism on skin collagen. *Maturitas* **33**, 239–247 (1999).
36. Morales, D. E. *et al.* Estrogen promotes angiogenic activity in human umbilical vein endothelial cells in vitro and in a murine model. *Circulation* **91**, 755–763 (1995).
37. Caliceti, C. *et al.* 17β-estradiol enhances signalling mediated by VEGF-A-delta-like ligand 4-notch1 axis in human endothelial cells. *PloS One* **8**, e71440 (2013).
38. Notas, G., Kampa, M. & Castanas, E. G protein-coupled estrogen receptor in immune cells and its role in immune-related diseases. *Front. Endocrinol.* **11**, 579420 (2020).
39. Wang, D. *et al.* Inflammation in mice ectopically expressing human pyogenic arthritis, pyoderma gangrenosum, and acne (PAPA) syndrome-associated PSTPIP1 A230T mutant proteins. *J. Biol. Chem.* **288**, 4594–4601 (2013).

40. Wang, C. *et al.* Membrane estrogen receptor regulates experimental autoimmune encephalomyelitis through up-regulation of programmed death 1. *J. Immunol.* **182**, 3294 (2009).
41. Ashcroft, G. S. *et al.* Estrogen modulates cutaneous wound healing by downregulating macrophage migration inhibitory factor. *J. Clin. Invest.* **111**, 1309–1318 (2003).
42. Rodenas, M. C. *et al.* G protein-coupled estrogen receptor 1 regulates human neutrophil functions. *Biomed. Hub* **2**, 1–13 (2017).
43. Kim, S. Y. & Nair, M. G. Macrophages in wound healing: Activation and plasticity. *Immunol. Cell Biol.* **97**, 258–267 (2019).
44. Rettew, J. A., McCall, S. H. IV. & Marriott, I. GPR30/GPER-1 mediates rapid decreases in TLR4 expression on murine macrophages. *Mol. Cell. Endocrinol.* **328**(1–2), 87–92 (2010).
45. Blasko, E. *et al.* Beneficial role of the GPR30 agonist G-1 in an animal model of multiple sclerosis. *J. Neuroimmunol.* **214**, 67–77 (2009).
46. Nosbaum, A. *et al.* Regulatory T cells facilitate cutaneous wound healing. *J. Immunol. Baltim. Md* **1950**(196), 2010–2014 (2016).
47. Ramirez, H., Patel, S. B. & Pastar, I. The role of TGFβ signaling in wound epithelialization. *Adv. Wound Care* **3**, 482–491 (2014).
48. Sanjabi, S., Oh, S. A. & Li, M. O. Regulation of the immune response by TGF-β: From conception to autoimmunity and infection. *Cold Spring Harb. Perspect. Biol.* **9**, 22236 (2017).
49. Ouyang, W., Beckett, O., Ma, Q. & Li, M. O. Transforming growth factor-beta signaling curbs thymic negative selection promoting regulatory T cell development. *Immunity* **32**, 642–653 (2010).
50. Brunsing, R. L. & Prossnitz, E. R. Induction of interleukin-10 in the T helper type 17 effector population by the G protein coupled estrogen receptor (GPER) agonist G-1. *Immunology* **134**, 93–106 (2011).
51. Brunsing, R. L., Owens, K. S. & Prossnitz, E. R. The G protein-coupled estrogen receptor (GPER) agonist G-1 expands the regulatory T-cell population under TH17-polarizing conditions. *J. Immunother. Hagerstown Md* **1997**(36), 190–196 (2013).
52. Leahy, M. J. *et al.* Biophotonic methods in microcirculation imaging. *Med. Laser Appl.* **22**, 105–126 (2007).
53. McGuire, P. G. & Howdieshell, T. R. The importance of engraftment in flap revascularization: Confirmation by laser speckle perfusion imaging. *J. Surg. Res.* **164**, e201–e212 (2010).
54. Ostle, B. & Malone, L. *Statistics in Research* (Iowa State University Press, Ames, 1988).

Author contributions

Conceptualization: ERP, TRH; Methodology: HJH, ERP, TRH; Investigation: RMC, JSB, GS, TRH; Data Presentation, Analysis and Interpretation: RFK, OQCD, MAA, ERP, TRH; Statistical Analyses: VSP; Writing—original draft: RFK, OQCD, MAA, ERP, TRH; Writing—review & editing: all authors.

Funding

E.R.P. is supported by grants from the US National Institutes of Health (R01 CA163890 and R01 CA194496) from Dialysis Clinic, Inc., and by the UNM Comprehensive Cancer Center (NIH P30 CA118100), and the Autophagy, Inflammation and Metabolism (AIM) Center of Biomedical Research Excellence (CoBRE, NIH P20 GM121176). R.F.K. is supported by the UNM Cardiovascular Research Training Program pre-doctoral fellowship (NIH T32HL007736) and by a grant from NIDDK (NIH F31DK136330). R.M.C. is supported by the UNM Clinical and Translational Science Center (NIH UL1TR001449) through the UNM KL2 Scholars Program (KL2TR001448).

Competing interests

ERP holds a patent on small molecules regulators of GPER activity. All other authors declare that they have no competing interests.

Additional information

Supplementary Information The online version contains supplementary material available at https://doi.org/10.1038/s41598-024-68620-3.

Correspondence and requests for materials should be addressed to E.R.P. or T.R.H.